Incremental Volt/Var Control for Distribution Networks via Chance-Constrained Optimization

Antonin Colot*, Elisabetta Perotti*, Mevludin Glavic, and Emiliano Dall'Anese

***Abstract*—This paper considers an incremental Volt/Var control scheme for distribution systems with high integration of inverter-interfaced distributed generation (such as photovoltaic systems). The incremental Volt/Var controller is implemented with the objective of minimizing reactive power usage while maintaining voltages within safe limits sufficiently often. To this end, the parameters of the incremental Volt/Var controller are obtained by solving a chance-constrained optimization problem, where constraints are designed to ensure that voltage violations do not occur more often than a pre-specified probability. This approach leads to cost savings in a controlled, predictable way, while still avoiding significant over- or under-voltage issues. The proposed chance-constrained problem is solved using a successive convex approximation method. Once the gains are broadcast to the inverters, no additional communication is required since the controller is implemented locally at the inverters. The proposed method is successfully tested on a low-voltage 42-nodes network.**

***Index Terms*—Incremental Volt/Var, distributed energy resources, distribution networks, chance-constrained optimization.**

I. Introduction

The increasing integration of distributed energy resources (DERs) is driving a paradigm shift in electrical power networks, moving away from centralized power plants and embracing decentralized energy systems. The growing share of inverter-interfaced renewable energy resources (RESs) in the electricity production mix, aimed to meet climate targets, poses a number of challenges on all aspects of electrical distribution networks (DNs), ranging from the planning to the real-time control [1], [2]. The goal of this paper is to address the voltage regulation problem in DNs by leveraging inverters' capabilities.

Literature Review. Traditionally, voltage regulation in DNs was achieved using load tap changers or switchgears. However, the increasing variability introduced by DERs can shorten their lifespan, and they may become insufficient to resolve voltage issues [3]. On the other hand, continuous improvements in power electronics converters create new possibilities for the control of DERs [4], enabling new tools for voltage regulation. The real-time control of DERs' powers can be categorized based on the control architecture. In a centralized approach, the system operator determines the DERs' power injections by solving a given instance of the optimal power flow (OPF) problem. The central controller needs a precise knowledge of the network, which may be hard to achieve in practice [5]. Even though recent feedback-based methods [6], [7] do not require perfect knowledge of non-controllable power injections, they rely on a communication infrastructure that is not present in existing DNs. In this paper, we focus on decentralized strategies, which offer simplicity and low implementation cost since they rely only on local measurements to perform control actions [8], [9].

Volt/Var controllers determine reactive power injections from, e.g., a static function of the local voltage measurements. The slopes of individual Volt/Var curves can be tuned to achieve various objectives by solving appropriate optimization problems [10]. Since these static feedback laws can lead to oscillatory behaviors [11], incremental strategies, based on voltage measurements and the past reactive power setpoint [12], are generally favored. Chance-constrained approaches to design optimal rules for *non*-incremental Volt/Var control are proposed in [13], [14]. These works consider a separate set of gains for each DER. This may be challenging in practice, as it requires knowledge of each DER location and an advanced communication infrastructure to properly dispatch the gains.

We also mention some representative works in the context of data-driven methods to learn a Volt/Var controller [15]. For learning-based strategies, it is often difficult to analyze the closed-loop stability [16]. Some exceptions are, e.g. [17], [18]; however, the controllers in these works do not minimize reactive power usage, potentially causing additional losses in the DN. In [19], closed-loop stability for a general class of Volt/Var controllers is guaranteed but historical data are needed for training the learning-based controllers. In the context of learning-based Volt/Var, however, it is difficult to account for network topology changes. Indeed, changes in topology may require collecting new data and re-training learning-based con-

* Equal contribution of the authors.

This work was supported in part by the National Science Foundation (NSF) awards 1941896. The work of E. Perotti was supported by Schmidt Science Fellows, in partnership with the Rhodes Trust. The work of A. Colot was supported by the Research Fellow Fellowship of the F.R.S-FNRS.

A. Colot and M. Glavic are with the Montefiore Institute, University of Liège (email: antonin.colot@uliege.be; mevludin.glavic@uliege.be).

E. Perotti and E. Dall'Anese are with the Department of ECEE, University of Colorado Boulder (email: elisabetta.perotti@colorado.edu; emiliano.dallanese@colorado.edu).

trollers, which is time-consuming. In [20], authors propose a linear Volt/Var controller and a methodology for adapting the controller to varying network topologies. However, this requires solving multiple instances of the OPF.

Statement of Contributions: We design a local incremental Volt/Var controller scheme that allows to specify the maximum amount of voltage violation that is tolerated. Fig. 1 illustrates the key steps of our approach. We formulate a chance-constrained optimization problem to ensure that voltage violations cannot occur more often than according to a given, prefixed probability. To the authors' knowledge, this is the first work that relies on chance-constrained optimization to determine the gains of an incremental Volt/Var controller. In particular, we consider a single set of gains suitable for all DERs, thus keeping the offline communication infrastructure requirements low.

With respect to a standard Volt/Var controller, this approach aims to minimize the generator's reactive power injections. The controller gains are determined in advance based on forecast data for power generation and loads. There is no need of historical data of any type. Therefore, not only can our approach easily handle planned topology changes but, even in case of unplanned changes, it is still reliable since network conditions are taken into account as feedback. To account for a variety of possible distributions of the forecasting errors, a conservative approximation of the chance constraints is derived [21]. Our approach uses an algorithm based on Successive Convex Approximation (SCA) methods [22] to derive a convex, and therefore tractable formulation of our chance-constrained problem.

Outline: In Section II, we define the DN model and formulate the problem. Section III introduces our incremental local Volt/Var controller and analyses its stability. Section IV presents a strategy to determine the controller gains that optimize the performance of our controller. Section V provides details regarding the implementation of the feedback controllers. Numerical simulations in Section VI compare the proposed approach to benchmark methods. Section VII concludes the paper.

II. Problem formulation

A. Power system model

Consider a balanced three-phase power distribution network[1] with $N+1$ nodes and hosting G DERs. The node 0 is taken to be the point of common coupling, while $\mathcal{N} := \{1, ..., N\}$ is the set of remaining nodes. We consider a phasor model of the single-phase equivalent DN where we define $u_k = v_k e^{j\delta_k} \in \mathbb{C}$ the voltage at node k. The voltage at node 0 is set to $u_0 = V_0$. Using Ohm's and Kirchhoff's laws, one has the usual relationship:

$$\mathbf{s} = \mathsf{diag}(\mathbf{u})(\mathbf{y}^* V_0 + Y^* \mathbf{u}^*), \tag{1}$$

where $\mathbf{u} := \{u_k\}_{k\in\mathcal{N}}$ collect the voltages at every node, and $\mathbf{s} = \mathbf{p}_{\text{av}} - \mathbf{p}_{\text{l}} + j(\mathcal{A}\widetilde{\mathbf{q}} - \mathbf{q}_{\text{l}}) \in \mathbb{C}^N$ is the net power injection at nodes $n \in \mathcal{N}$. The network bus admittance matrix is partitioned such that $\mathbf{y} \in \mathbb{C}^N, Y \in \mathbb{C}^{N\times N}$. We define $\mathbf{p}_{\text{av}}, \mathbf{p}_{\text{l}}, \mathbf{q}_{\text{l}} \in \mathbb{R}^N$ as the vectors collecting the non-controllable active power injection, the active and reactive power consumption at nodes $n \in \mathcal{N}$, respectively. We define $\widetilde{\mathbf{q}} \in \mathbb{R}^G$ as the vector collecting the controllable reactive power of the G DERs. The matrix $\mathcal{A} \in \mathbb{R}^{N\times G}$ maps the index of a DER to the node where it is located.

Equation (1) describes the power flow equations. For a given vector of net power injection $\mathbf{s}$, one can solve this non-linear system of equations using numerical methods to find the vector of voltage phasors $\mathbf{u}$. Notice that the system of equations (1) may have zero, one or many solutions. For the rest of this paper, we make the following assumption.

Assumption 1 (Existence and uniqueness of a practical solution of the power flow equations): There exists at least one solution to the power flow equations (1). If multiple solutions exist, we only consider the *practical* solution, i.e., in the neighborhood of the nominal voltage profile, we pick the high voltage, and small line currents solution. □

Let us define $\mathbf{z} := (\mathbf{p}_{\text{av}}, \mathbf{p}_{\text{l}}, \mathbf{q}_{\text{l}})$ as the concatenation of the non-controllable powers, the algebraic map $H := \mathbb{R}^{G+3N} \to \mathbb{R}^N$ and $\mathbf{v} := \{v_k\}_{k\in\mathcal{N}}$ the vector collecting the voltage magnitudes at every node. For convenience, we denote $\mathbf{v} = H(\widetilde{\mathbf{q}}, \mathbf{z})$ where H relates the net power injections to the *practical* solution of the power flow equations defined in (1). Although the analytical form of the map H is not known, its existence and uniqueness have been discussed for balanced [23], [24] and multi-phase DNs [25].

B. Problem setup

The deployment of inverter-interfaced generation in DNs might induce voltage quality issues. However, DERs can also be used to provide voltage regulation services via, e.g., reactive power compensation. Ideally, one wants to minimize the total reactive power usage while maintaining voltages inside a given feasible set. We formulate an optimal reactive power flow problem as follows:

$$\begin{aligned} (\text{P0}(t)) \quad & \min_{\widetilde{\mathbf{q}}\in\mathcal{Q}} \quad f(\widetilde{\mathbf{q}}) \\ & \quad \text{s.t.} \quad H(\widetilde{\mathbf{q}}, \mathbf{z}(t)) \in \mathcal{V}, \end{aligned} \tag{2}$$

[1] *Notation. Upper-case (lower-case boldface) letters are used for matrices (column vectors); $(.)^\top$ denotes the transposition, $(.)^*$ denotes the complex conjugate and $(.)^{-1}$ denotes the inverse matrix; j the imaginary unit and $|.|$ the absolute value of a number. If we consider a given vector $\mathbf{x} \in \mathbb{R}^N$, $\mathsf{diag}(\cdot)$ returns a $N \times N$ matrix with the element of $\mathbf{x}$ in its diagonal. For vectors $\mathbf{x} \in \mathbb{R}^n$ and $\mathbf{u} \in \mathbb{R}^m$, $\|\mathbf{x}\|$ denotes the ℓ_2-norm and $(\mathbf{x}, \mathbf{u}) \in \mathbb{R}^{n+m}$ denotes their vector concatenation. We denote as $\mathbf{0}$ a vector with all zeros (the dimensions will be clear from the context). We denote $\mathbb{R}_{>0}, \mathbb{R}_{\geq 0}$ and $\mathbb{R}_{\leq 0}$ the set of strictly positive, positive and negative real numbers. $\mathbb{1}$ denotes the $N \times 1$ column vector and $\mathbb{I}$ the $N \times N$ identity matrix.*

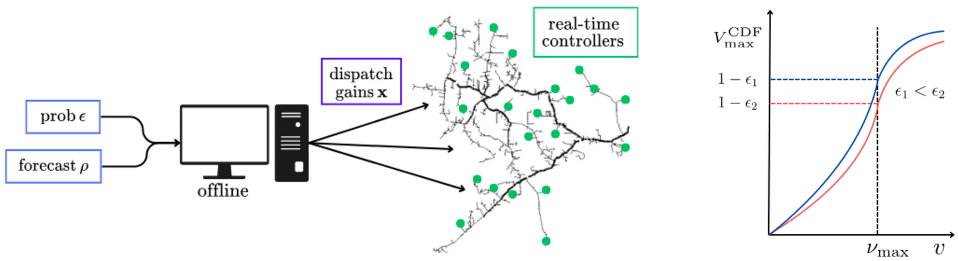

(a) (b)

Fig. 1: (a) Proposed voltage regulation strategy. Based on the forecast $\boldsymbol{\rho}$ and the probability ϵ to violate voltage limits, the controller gains $\mathbf{x}$ are computed offline and then dispatched to the controllable DERs. (b) Illustrative explanation of the impact of the parameter ϵ on the total amount of voltage violations. A smaller ϵ results in a more constrained optimization problem and therefore in fewer voltage violations.

where $\mathcal{Q} \subset \mathbb{R}^G$ is the set of feasible values for the reactive powers, $\mathcal{V} \subset \mathbb{R}^N$ is the set of feasible values for voltage magnitudes, and $f : \mathbb{R}^G \to \mathbb{R}$ is a differentiable cost function. Notice that (P0(t)) is a time-varying optimization problem. Indeed, the non-controllable power injections $\mathbf{z}(t)$ vary with time as they depend on users' habits and weather conditions. Therefore, also the optimal reactive power injections are time dependent; their time-scale is determined by the variability of the non-controllable power injections and is usually within seconds [26]. However, collecting data, solving problem (P0(t)) and broadcasting the setpoints to the inverters every second is challenging because of the non-linear nature of the power flow equations (1) represented by H, and the communication burden associated with large DNs. This paper aims to solve the following problem.

Problem 1: Design feedback controllers to approximate the solution of (P0(t)) with limited computational resources and in a decentralized fashion, i.e., each controller uses only local voltage measurements to compute its reactive power output and the operation does not necessitate continuous communications with neighbours or a centralized entity. □

To outline the proposed framework, we consider the case where there is one DER per node in the network and the map H does not change over time. Additionally, we make the following assumption.

Assumption 2 (Feasibility): For any $\mathbf{q} \in \mathcal{Q}$, there exists a solution such that $\mathbf{v}(t) \in \mathcal{V}$. □

This assumption ensures that there is enough reactive power reserve to regulate the voltages. We will review this assumption and our setup choices later, and discuss how they could be relaxed.

III. Design of feedback controllers

Within the next section, we identify three different time scales. In order from the shortest to the longest, they correspond to the time scales that characterize the following events: i) controller law updates, ii) forecast updates and iii) controller gains updates.

a) Incremental Volt/Var control: To begin with, we consider only the shortest time scale, which is related to the controller law updates. Let us discretize the temporal domain as $t = k\tau$, where $k \in \mathbb{N}_+$ and $\tau \in \mathbb{R}_{>0}$ is a given time interval, small enough to resolve variations in the time-dependent disturbances, i.e., less than a second. We consider the following feedback controller:

$$\mathbf{q}_{k+1} = \mathbf{q}_k + \eta(\mathbb{1} - \boldsymbol{\nu}_k) - (1-\eta)\alpha\mathbf{q}_k, \tag{3}$$

where $\alpha \in \mathbb{R}_{\geq 0}$, $\eta \in [0, 1]$, and $\boldsymbol{\nu}_k = X\mathbf{q}_k + \boldsymbol{\rho}_k$ with $X \in \mathbb{R}^{N\times N}$ is a linear approximation of the power flow equations and $\boldsymbol{\rho}_k = H(\mathbf{0}, \mathbf{z}_k)$ denotes the voltage profile obtained by setting the controllable reactive powers to 0. The linearized power flow equations can be derived from the bus injection model [26], or from the branch flow model [27]. For the rest of this paper, we consider the linearized power flow equations based on the branch flow model [28], since it guarantees X being positive definite [29]. This approximation has been used in [16], [27], and its quality has been discussed in [29]. Notice that $\boldsymbol{\rho}_k = H(\mathbf{0}, \mathbf{z}_k)$ is derived from the true power flow equations. Substituting this approximation in (3), the controller can be written as:

$$\mathbf{q}_{k+1} = A(\eta, \alpha)\mathbf{q}_k + B(\eta, \boldsymbol{\rho}), \tag{4}$$

where $A(\eta, \alpha) := (1 - (1-\eta)\alpha)\mathbb{I} - \eta X$ and $B(\eta, \boldsymbol{\rho}) := \eta(\mathbb{1} - \boldsymbol{\rho})$.

b) Existence and uniqueness of the equilibrium: Denoting $\boldsymbol{\rho} = \boldsymbol{\rho}_k$ for a given k, the equilibrium for (4) is defined as:

$$\begin{aligned} \mathbf{q}^* &= \left[\eta X + (1-\eta)\alpha\mathbb{I}\right]^{-1} \eta(\mathbb{1} - \boldsymbol{\rho}) \\ \boldsymbol{\nu}^* &= X\left[\eta X + (1-\eta)\alpha\mathbb{I}\right]^{-1} \eta(\mathbb{1} - \boldsymbol{\rho}) + \boldsymbol{\rho}. \end{aligned} \tag{5}$$

Since X is positive definite and $\alpha \in \mathbb{R}_{\geq 0}$, $\eta \in [0, 1]$, the matrix $\eta X + (1-\eta)\alpha\mathbb{I}$ in (5) is always invertible and the equilibrium is unique. One can check that for $\eta = 0$ and $\alpha > 0$, $\mathbf{q}^* = \mathbf{0}$ and $\boldsymbol{\nu}^* = \boldsymbol{\rho}$, while for $\eta > 0$ and $\alpha = 0$ or $\eta = 1$, $\mathbf{q}^* = X^{-1}(\mathbb{1} - \boldsymbol{\rho})$ and $\boldsymbol{\nu}^* = \mathbb{1}$.

Increasing the gain α decreases the use of reactive power, while increasing the gain η steers the voltage magnitudes to the nominal voltage profile.

c) Stability analysis: The controller (4) is asymptotically stable if and only if $\rho(A(\eta,\alpha)) < 1$, where $\rho(\cdot)$ denotes the spectral radius. This condition is verified if:

$$\mathbf{0} < (1-\eta)\alpha\mathbb{1} + \eta\boldsymbol{\lambda}_X < 2\mathbb{1}, \tag{6}$$

where $\boldsymbol{\lambda}_X \in \mathbb{R}^N$ is the vector containing the eigenvalues of the matrix X. Moreover the matrix X is positive definite by construction, and since η, α satisfy $\alpha \in \mathbb{R}_{\geq 0}$, $\eta \in [0,1]$, we always have $(1-\eta)\alpha\mathbb{1} + \eta\boldsymbol{\lambda}_X \geq \mathbf{0}$. The equality holds only if $\eta = \alpha = 0$, which guarantees a stable controller since $\mathbf{q}_{k+1} = \mathbf{q}_k$.

d) Multi-phase unbalanced distribution networks: DNs are often highly unbalanced, and may have different connection configurations (wye-connected or delta-connected). In order to study the stability properties of the controller (3) for unbalanced DNs, one would need to use a different approximation of the power flow equations, e.g., [25], [30]. In our formulation, we leverage the positive definite property of the matrix X to show the uniqueness and existence of the equilibrium, as well as the stability of the controller. To adapt this framework to unbalanced DNs, one would need to study the properties of the new matrix X to characterize the equilibrium and stability properties of the controller (3). However, as mentioned in [30], due to the structure of the distribution lines, X is often positive definite for unbalanced networks. In such cases, our methodology can be readily applied to multi-phase networks.

IV. Design of the Controller Gains

The performance of the controller (4) depends on the choice of η and α. In the following section, we introduce an optimization-based method to design the gains.

A. Time-varying formulation

Given a matrix X, a time-varying vector $\boldsymbol{\rho}_k = H(\mathbf{0}, \mathbf{z}_k)$, and feasible sets $\mathcal{Q}$ and $\mathcal{V}$, we formulate the following problem at time $k\tau$:

$$\begin{aligned}
(\mathrm{P1}_k) \quad \min_{\alpha\in\mathbb{R}_{\geq 0}, \eta\in[0,1]} \quad & \|\mathbf{q}_k(\alpha,\eta)\|^2 && \text{(7a)}\\
\text{s.t.} \quad & \mathbf{q}_k(\alpha,\eta) \in \mathcal{Q} && \text{(7b)}\\
& X\mathbf{q}_k(\alpha,\eta) + \boldsymbol{\rho}_k \in \mathcal{V} && \text{(7c)}\\
& (1-\eta)\alpha\mathbb{1} + \eta\boldsymbol{\lambda}_X < 2\mathbb{1} && \text{(7d)}
\end{aligned}$$

where $\mathbf{q}_k(\alpha,\eta) = [\eta X + (1-\eta)\alpha\mathbb{I}]^{-1}\eta(\mathbb{1} - \boldsymbol{\rho}_k)$ is a non-linear function of η and α. For a given time $k\tau$, the goal is to minimize the reactive power usage $\|\mathbf{q}_k(\alpha,\eta)\|^2$, while satisfying operational constraints, by appropriately selecting the gains η and α.

An alternative formulation of problem $(\mathrm{P1}_k)$ can be derived using an appropriate change of variable. We introduce the optimization variable $\mathbf{x} = [\frac{\alpha}{\eta}, -\alpha]^\top \in \mathbb{R}_{\geq 0} \times \mathbb{R}_{\leq 0}$, rewrite $\mathbf{q}_k(\mathbf{x}) = \left[X + \mathbf{1}^\top\mathbf{x}\mathbb{I}\right]^{-1}(\mathbb{1} - \boldsymbol{\rho}_k)$, specify $\mathcal{Q}$ and $\mathcal{V}$ in terms of box constraints, and reformulate the problem $(\mathrm{P1}_k)$ as

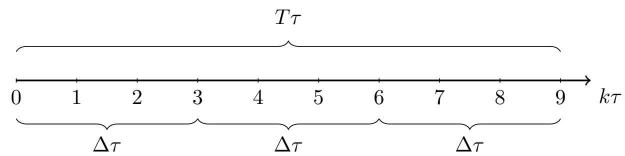

Fig. 2: Comparison between different time scales of the problem, assuming $\tau = 1s$.

$$\begin{aligned}
(\mathrm{P2}_k) \quad \min_{\mathbf{x}} \quad & h_0^k(\mathbf{x}) \\
\text{s.t.} \quad & h_i^k(\mathbf{x}) \leq 0 \quad \forall i \in \{1, ..., 8\}
\end{aligned} \tag{8}$$

where

$$\begin{aligned}
& h_0^k(\mathbf{x}) = \|\mathbf{q}_k(\mathbf{x})\|^2, \quad h_1^k(\mathbf{x}) = \mathbf{q}_k(\mathbf{x}) - \mathbf{q}_{\max}, \\
& h_2^k(\mathbf{x}) = -\mathbf{q}_k(\mathbf{x}) + \mathbf{q}_{\min}, \\
& h_3^k(\mathbf{x}) = X\mathbf{q}_k(\mathbf{x}) + \boldsymbol{\rho}_k - \boldsymbol{\nu}_{\max}, \\
& h_4^k(\mathbf{x}) = -X\mathbf{q}_k(\mathbf{x}) - \boldsymbol{\rho}_k + \boldsymbol{\nu}_{\min}, \\
& h_5(\mathbf{x}) = \left(\mathbf{1}^\top\mathbf{x} - 2\right)\mathbb{1} + \boldsymbol{\lambda}_X, \\
& h_6(\mathbf{x}) = -\mathbf{1}^\top\mathbf{x}, \quad h_7(\mathbf{x}) = -x_1, \quad h_8(\mathbf{x}) = x_2,
\end{aligned} \tag{9}$$

with x_1, x_2 scalar components of $\mathbf{x}$ and $\mathbf{1} = [1,1]^\top \in \mathbb{R}^2$. The objective function h_0 is a scalar function, as well as h_6, h_7 and h_8. All other constraint functions h_i with $i = 1, ..., 5$ are vector-valued. Function $h_5(\mathbf{x})$ gives a tighter bound on (7d) with the equality reached for $\eta = 1$, such that the controller gains derived from $(\mathrm{P2}_k)$ ensure asymptotic stability of the controller defined in (3) as long as $\eta < 1$. The conditions $\eta < 1$ is always verified as $\eta = 1$ implies $\boldsymbol{\nu}^* = \mathbb{1}$ which leads to a suboptimal solution (unless $\boldsymbol{\nu}_{\min} = \boldsymbol{\nu}_{\max} = \mathbb{1}$).

As explained in Section II-B, collecting measurements at every nodes, solving $(\mathrm{P2}_k)$ and then dispatching the controller gains to the controllable DERs in *real-time* is unfeasible because of the communication burden and the computational time required to solve $(\mathrm{P2}_k)$. One could envision solving $(\mathrm{P2}_k)$ *offline* for every time $k\tau$ using forecasts of $\boldsymbol{\rho}_k$. However, it is not realistic to have such frequent forecast updates, since τ should be sufficiently small to cope with the DN dynamics. Furthermore, $\boldsymbol{\rho}_k$ is affected by large uncertainties as it inherits them from $\mathbf{z}_k$ through $\boldsymbol{\rho}_k = H(\mathbf{0}, \mathbf{z}_k)$. Moreover, we would like to find optimal controller gains η and α over a longer time period, to avoid broadcasting new values at every time $k\tau$, or to avoid storing a large number of gains in each controller. In the next section we address this issue by reformulating our problem in a chance-constrained fashion.

B. Chance-constrained formulation

Given that our forecast $\boldsymbol{\rho}_k = H(\mathbf{0}, \mathbf{z}_k)$ is subject to uncertainty in the vector $\mathbf{z}_k$, we implement probabilistic constraints in our optimization problem in order to enforce voltage regulation with prescribed probability. The available DERs' powers at time $k\tau$ are modeled by $\mathbf{p}_{\mathrm{av},k} = \bar{\mathbf{p}}_{\mathrm{av},k} + \boldsymbol{\delta}_{\mathrm{av},k}$, while the active and reactive loads are expressed as $\mathbf{p}_{\mathrm{l},k} = \bar{\mathbf{p}}_{\mathrm{l},k} + \boldsymbol{\delta}_{\mathrm{pl},k}$ and $\mathbf{q}_{\mathrm{l},k} = \bar{\mathbf{q}}_{\mathrm{l},k} + \boldsymbol{\delta}_{\mathrm{ql},k}$, respectively. Writing $\boldsymbol{\delta}_k := (\boldsymbol{\delta}_{\mathrm{av},k}, \boldsymbol{\delta}_{\mathrm{pl},k}, \boldsymbol{\delta}_{\mathrm{ql},k})$, and $\bar{\mathbf{z}}_k := (\bar{\mathbf{p}}_{\mathrm{av},k}, \bar{\mathbf{p}}_{\mathrm{l},k}, \bar{\mathbf{q}}_{\mathrm{l},k})$, we have $\boldsymbol{\rho}_k = H(\mathbf{0}, \bar{\mathbf{z}}_k + \boldsymbol{\delta}_k)$ where $\boldsymbol{\delta}_k$ follows a given distribution function.

It is reasonable to assume that a new forecast for $\boldsymbol{\rho}_k$ will be available after a certain time interval $\Delta\tau$ with $\Delta \in \mathbb{N}_+$ (for example, Δ could be such that $\Delta\tau = 15$ minutes). Concretely, this means that within a time window of duration $\Delta\tau$, $\boldsymbol{\rho}_k$ will be the same, regardless of the value of the index k. Therefore, we will drop the index k in the following, and consider $\boldsymbol{\rho}^m$ instead to underline that the forecast $\boldsymbol{\rho}^m$ will be updated at each time $t = m\Delta\tau$ with $m \in \mathbb{N}_+$. This introduces a longer time scale, whose magnitude is related to how often forecast updates occur.

Ultimately, our goal is to determine controller gains to be deployed over an even longer time interval $T\tau$ where $T = b\Delta$ with $b \in \mathbb{N}_+$, e.g., b is such that $T\tau = 1$ hour. Fig. 2 provides a visual representation of the relationship between the three different time scales relevant to this problem.

We consider an extension of (P2$_k$) as a multi-period optimization problem:

$$\begin{aligned}
\text{(P3)} \quad \min_{\mathbf{x}} \quad & \sum_{m=1}^{b} \mathbb{E}\{h_0(\mathbf{x};\boldsymbol{\rho}^m)\} \\
\text{s.t.} \quad & \Pr\{h_{i,n}(\mathbf{x};\boldsymbol{\rho}^m) \le 0\} \ge 1-\epsilon_i \\
& \quad \forall i \in \{1,2,3,4\}, n \in \mathcal{N}, m \in \{1,..,b\} \\
& h_i(\mathbf{x}) \le 0 \quad \forall i \in \{5,6,7,8\}
\end{aligned} \tag{10}$$

where we sum over b intervals of magnitude Δ, corresponding in total to a period of time $T\tau$. Notice that for $b = 1$, we recover a single-interval formulation. $\Pr\{A\}$ denotes probability of an event A to happen, meaning that in problem (P3) the constraints $h_i(\mathbf{x};\boldsymbol{\rho}^m) \le 0$ for $i = 1,2,3,4$ are satisfied with a probability $1-\epsilon_i$, where $\epsilon_i \in (0,1)$. Solving problem (P3) for the optimization variable $\mathbf{x}$, we can retrieve the values of the gains α and η to be deployed during a time interval of length $T\tau$. When following this approach we lose optimality in exchange for convenience: (P3) can be solved offline using a coarser forecast and controller gains are designed to cover wider time windows, which is a great advantage from a practical point of view. Finally, notice that the objective function $h_0(\mathbf{x};\boldsymbol{\rho}^m)$ also depends on $\boldsymbol{\rho}^m$, thus we minimize its expected value.

We seek a tractable approximation for the chance constraints in (10) since we do not know the probability distribution function of $\boldsymbol{\delta}_k$, neither the map H. The chance constraints to be approximated are of the form $\Pr\{h(\mathbf{x};\boldsymbol{\rho}) \le 0\} \ge 1-\epsilon$, where the function $h(\mathbf{x},\boldsymbol{\rho})$ depends on the optimization variable $\mathbf{x}$ and the random vector $\boldsymbol{\rho}$. Consider $\psi(x) = [1+x]_+$, where $[x]_+ := \max\{x,0\}$, a so-called generating function $\psi : \mathbb{R} \to \mathbb{R}$ nonnegative, nondecreasing, and convex that satisfies the conditions $\psi(x) > \psi(0)\, \forall x > 0$ and $\psi(0) = 1$. Given a positive scalar $z > 0$, we have that the following bound holds for all $z > 0$ and $\mathbf{x}$ [21]:

$$\inf_{z\in\mathbb{R}} \{\mathbb{E}_{\boldsymbol{\rho}}\{[h(\mathbf{x},\boldsymbol{\rho}) + z]_+\} - z\epsilon\} \le 0. \tag{11}$$

Each probabilistic constraint in (10) will be replaced by the approximation (11):

$$\mathbb{E}_{\boldsymbol{\rho}^m}\{[h_{i,n}(\mathbf{x};\boldsymbol{\rho}^m) + u_{i,n}^m]_+\} - u_{i,n}^m\epsilon \le 0, \tag{12}$$

where $u_{i,n}^m$ are real and positive auxiliary optimization variables. Moreover, since the max operator $[.]_+$ is not differentiable, we replace it with a smooth approximation and define:

$$\begin{aligned}
& g_{i,n}(\mathbf{x}, u_{i,n};\boldsymbol{\rho}^m) = \\
& \quad \frac{1}{2}\left(h_{i,n}(\mathbf{x}) + u_{i,n} + \sqrt{\xi^2 + (h_{i,n}(\mathbf{x}) + u_{i,n})^2}\right) - u_{i,n}\epsilon \\
& \quad \forall i \in \{1,2,3,4\}, n \in \mathcal{N}, m \in \{1,..,b\}
\end{aligned} \tag{13}$$

with ξ small and non-zero. Differentiability of the functions g_i will be required later in Section IV-C where we will convexify problem (P4) introduced below. The expected values in (12) can be estimated empirically via sample averaging for a sufficiently large number of samples N_s, leading to a new formulation of the optimization problem:

$$\text{(P4)} \min_{\mathbf{x}, u_{i,n}^m} \quad \sum_{m=1}^{b} \quad \frac{1}{N_s}\sum_{s=1}^{N_s} h_0(\mathbf{x};\boldsymbol{\rho}^m[s]) \tag{14a}$$

$$\begin{aligned}
\text{s.t.} \quad & \frac{1}{N_s}\sum_{s=1}^{N_s} g_{i,n}(\mathbf{x}, u_{i,n}^m;\boldsymbol{\rho}^m[s])) \le 0 \\
& \quad \forall i \in \{1,2,3,4\}, n \in \mathcal{N}, m \in \{1,..,b\}
\end{aligned} \tag{14b}$$

$$h_i(\mathbf{x}) \le 0 \quad \forall i \in \{5,6,7,8\} \tag{14c}$$

where we will draw N_s samples $\boldsymbol{\rho}^m[s]_{s=1}^{N_s}$ of the random vector $\boldsymbol{\rho}^m$. Problem (P4) constitutes a conservative approximation of the initial chance constrained problem (P3), meaning that an optimal solution to (P4) is a feasible suboptimal solution to (P3).

C. Solution via successive convex approximation

At first one might try to solve problem (P4) with any software package for nonlinear optimization. However, it is not straightforward to implement the inverse matrix contained in $\mathbf{q}(\mathbf{x})$ in a computationally efficient way. Therefore, we seek a different strategy that may be computationally more affordable. In particular, we will leverage the algorithm proposed in [22] which follows the ideas of SCA methods. More specifically, the method solves a sequence of strongly convex inner approximation of an initial non-convex problem. In particular, each intermediate problem is strongly convex and can be written as:

$$
\begin{aligned}
(\text{P5}(\mathbf{x}_p)) \min_{\mathbf{x}, u_{i,n}^m} \quad & \sum_{m=1}^{b} \frac{1}{N_s} \sum_{s=1}^{N_s} \widetilde{h}_0(\mathbf{x}; \boldsymbol{\rho}^m[s], \mathbf{x}_p) \\
\text{s.t.} \quad & \frac{1}{N_s} \sum_{s=1}^{N_s} \widetilde{g}_{i,n}(\mathbf{x}, u_{i,n}^m; \boldsymbol{\rho}^m[s], \mathbf{x}_p) \leq 0 \\
& \quad \forall i \in \{1,2,3,4\}, n \in \mathcal{N},\ m \in \{1,..,b\} \\
& h_i(\mathbf{x}) \leq 0 \quad \forall i \in \{5,6,7,8\}
\end{aligned} \tag{15}
$$

where $\widetilde{g}_{i,n}(\mathbf{x}, u_{i,n}^m; \boldsymbol{\rho}^m[s], \mathbf{x}_p)$ approximates $g_{i,n}(\mathbf{x}, u_{i,n}^m; \boldsymbol{\rho}^m[s])$ around $\mathbf{x} = \mathbf{x}_p$. For given samples $\boldsymbol{\rho}^m[s]$, the problem $(\text{P5}(\mathbf{x}_p))$ is solved for successive values of $\mathbf{x}_p$ until convergence. The surrogate functions in (15) are defined as:

$$
\begin{aligned}
\widetilde{h}_0(\mathbf{x}; \boldsymbol{\rho}^m[s], \mathbf{x}_p) = \|\mathbf{q}(\mathbf{x}_p) + (\mathbf{x} - \mathbf{x}_p)^\top \nabla \mathbf{q}(\mathbf{x}_p)\|^2 \\
+ \frac{d}{2}\|\mathbf{x} - \mathbf{x}_p\|^2
\end{aligned} \tag{16}
$$

and

$$
\begin{aligned}
& \widetilde{g}_{i,n}(\mathbf{x}, u_{i,n}^m; \boldsymbol{\rho}^m[s], \mathbf{x}_p) = \\
& \quad \frac{1}{2}\left(\widetilde{h}_{i,n}(\mathbf{x}) + u_{i,n}^m + \sqrt{\xi^2 + (\widetilde{h}_{i,n}(\mathbf{x}) + u_{i,n}^m)^2}\right) - u_{i,n}^m \epsilon \\
& \quad \forall i \in \{1,2,3,4\}, n \in \mathcal{N}, m \in \{1,..,b\}
\end{aligned} \tag{17}
$$

with

$$
\begin{aligned}
& \widetilde{h}_{i,n}(\mathbf{x}; \boldsymbol{\rho}^m[s], \mathbf{x}_p) = \\
& h_{i,n}(\mathbf{x}_p) + (\mathbf{x} - \mathbf{x}_p)^\top \nabla h_{i,n}(\mathbf{x}_p) + (\mathbf{x} - \mathbf{x}_p)^\top M_{i,n}(\mathbf{x} - \mathbf{x}_p) \\
& \quad \forall i \in \{1,2,3,4\}, n \in \mathcal{N}, m \in \{1,..,b\}
\end{aligned} \tag{18}
$$

where $M_{i,n} \in \mathbb{R}^{2\times 2}$ is derived to ensure that $\widetilde{h}_{i,n}(\mathbf{x}; \boldsymbol{\rho}^m[s], \mathbf{x}_p)$ is a global majorizer of $h_{i,n}(\mathbf{x}_p; \boldsymbol{\rho})$. To lighten the notation, we omit the $\boldsymbol{\rho}^m$ dependence on the RHS of equations (16–18) but recall that $\mathbf{q}(\mathbf{x}; \boldsymbol{\rho}) = \left[X + \mathbf{1}^\top \mathbf{x}\mathbb{I}\right]^{-1}(\mathbb{1} - \boldsymbol{\rho})$ with $\boldsymbol{\rho} = H(\mathbf{0}, \mathbf{z})$, and the functions $h_{i,n}(\mathbf{x}; \boldsymbol{\rho})$ are defined in equation (9). The surrogate functions $\widetilde{h}_0$, $\widetilde{g}_i$ and $\widetilde{h}_i$ defined in equations (16–18) satisfy the assumptions listed in [22], and are therefore suitable for the SCA method.

Next we present our algorithm to solve $(\text{P5}(\mathbf{x}_p))$. First, let us define the set $\mathcal{K}$ defined by equations (14c), i.e., the set defined by the convex constraints of problem (P4). Let us also define the set $\mathcal{X}$ defined by equations (14c) and (14b), such that $\mathcal{X} \subset \mathcal{K}$. Then, Algorithm 1 is guaranteed to converge towards a stationary solution of problem $(\text{P5}(\mathbf{x}_p))$ under the assumptions specified in [22].

Algorithm 1 *Optimal Gain Design via SCA*

Initialization: $\gamma_p \in (0,1]$, $\mathbf{x}_0 \in \mathcal{X}$. Set $p = 0$.
[1.] If $\|\mathbf{x}_p - \mathbf{x}_{p-1}\| < e$ with $e > 0$, then STOP.
[2.] Compute the solution $\mathbf{x}^*(\mathbf{x}_p)$ of $(\text{P5}(\mathbf{x}_p))$.
[3.] Set $\mathbf{x}_{p+1} = \mathbf{x}_p + \gamma_p(\mathbf{x}^*(\mathbf{x}_p) - \mathbf{x}_p)$
[4.] $p \leftarrow p + 1$ and go to step 1.

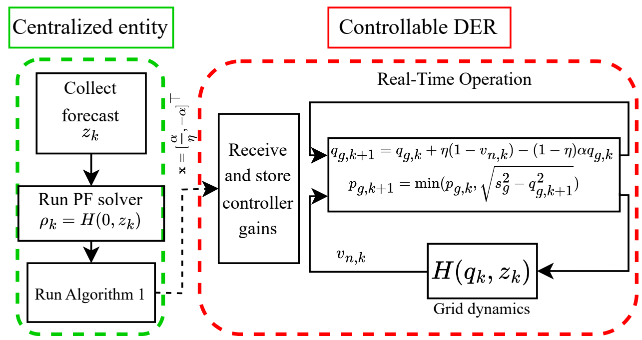

Fig. 3: Block diagram of the proposed framework.

V. Implementation of the Controllers

We assume that each controller is equipped with sensing capabilities, i.e., it is capable of measuring the voltage magnitudes at the node where it is located. For any given DER $g \in \mathcal{G}$ connected to node $n \in \mathcal{N}$, the following incremental Volt/Var control is implemented:

$$
q_{g,k+1} = q_{g,k} + \eta(1 - v_{n,k}) - (1-\eta)\alpha q_{g,k} \tag{19a}
$$

$$
p_{g,k+1} = \min\left(p_{g,k}, \sqrt{s_g^2 - q_{g,k+1}^2}\right), \tag{19b}
$$

with s_g the nominal rated size of DER g. Equation (19a) represents the reactive power update of DER g connected at node n. The approximated voltage $\nu_{n,k}$ written in the initial controller formulation (3) has been replaced by the voltage measurement $v_{n,k}$, which makes this controller fully decentralized (we no longer rely on the matrix X, and the impact of other DERs' reactive power is implicitly taken into account through the network feedback). Equation (19b) indicates that we prioritize reactive power over active power. By prioritizing reactive power over active power, we further mitigate overvoltage issues as the active power injection is reduced and reactive compensation is used. However, this induces active power curtailment which is costly. We will investigate this issue in the next section, where we will present our numerical results. The good behavior of the controller with reactive power prioritization is verified throughout simulations. We leave for future work the theoretical stability study of our controller when considering active power curtailment.

Fig. 3 illustrates the different stages of the framework proposed in this work. We compute the gains η and α for a given time interval $T\tau$ by solving the problem $(\text{P5}(\mathbf{x}_p))$ until convergence based on forecasts of $\mathbf{z}_k$. The samples

$\boldsymbol{\rho}^m[s]$ are generated by solving multiple power flows for different values of $\mathbf{z}_k = \bar{\mathbf{z}}_k + \boldsymbol{\delta}_k$, where $\boldsymbol{\delta}_k$ follows a given probability distribution function. The gains can be computed the day before deployment, or hours ahead depending on the forecast availability and the computational time required to solve (P5($\mathbf{x}_p$)) until convergence. They are then broadcast to the controllable DERs. Notice that we do not need to differentiate between DERs as the gains are the same for any DER connected to the network.

We are now ready to address the assumptions introduced in Section II-B. First, our current framework enforces one and only one DER per node. This requirement is rather restrictive, even though it has already been adopted in the literature, e.g. [27]. We can easily relax this assumption by considering only the entries of matrix X that correspond to the nodes where a controllable DER is located. The drawback is that we can only guarantee voltage satisfaction for a subset $\mathcal{N}_{\text{red}} \subset \mathcal{N}$ of nodes. However, the effect of other controllable devices can be embedded in the map H. For instance, on-load tap changers (OLTC) or switched capacitor banks can drive the forecast voltage profiles $\boldsymbol{\rho} = H(\mathbf{0}, \mathbf{z})$ inside the feasible set $\mathcal{V}$. Our methodology can be combined with other traditional regulation methods, and an optimal combination of slow acting controllers, such as OLTC, with our fast acting controllers is part of our future work. Furthermore, if multiple DERs are connected to the same node, one can aggregate the DERs and model them as one single device associated with one controller. The reactive power setpoint produced by controller (3) is then appropriately dispatched to the different DERs.

Second, in the present setup the network topology does not change with time. However, in our current framework, topological changes that can be forecast (because of maintenance or planned operation) can easily be integrated. Indeed, those changes impact the matrix X. By appropriately choosing the time interval $T\tau$ and recomputing X, one can derive gains that would be well adapted to this new network topology. This assumption is much harder to relax for learning-based methods such as the one proposed in [19] since it requires building new datasets, and learning new equilibrium functions, which can be time-consuming. When it comes to unplanned changes, e.g. sudden line tripping or unplanned operations, our controllers take into account the network conditions as a feedback, and do not worsen the situation. Nevertheless, evaluation of the robustness with respect to unplanned changes remains to be investigated in our future work.

Finally, Assumption 2 tackles the feasibility issue of the optimal reactive power flow problem. It may happen that, under our controller architecture, there is not enough reactive power reserve to satisfy the voltage constraints. This problem is implicitly addressed through our chance-constrained formulation. Indeed, increasing the value of ϵ enlarges the feasible set. For $\epsilon = 1$, the problem (P5($\mathbf{x}_p$)) is always feasible.

VI. Numerical experiments

We consider the low voltage network (0.4 kV) shown in Fig. 4a. We used a modified network from [31], in which photovoltaic power (PV) plants have been placed at each node, with inverter-rated size picked randomly among $\{20, 25, 31\}$ kVA. The DERs dynamics are not implemented, as they are considered to be much faster than the controller dynamics. This is a reasonable assumption because of the time-scale separation between the power system phenomena and the different control loops as mentioned in [16]. As such, when the controller update law produces a new reactive power setpoint, it is instantaneously implemented by the controllable DER. In this paper, we only consider PV plants as DERs, but any type of inverter-interfaced generation for which the reactive power can be controlled could be considered. Fig. 4b shows the aggregated loads and maximum available active power for PV plants throughout the day. The data is from the Open Power System Data[2], and have been modified to match the initial loads and PV plants nominal values present in the network. The reactive power demand is set such that the power factor is 0.95 (lagging). This represents a typical summer day, with high PV production. We will show that, under these conditions, the electrical DN undergoes both overvoltages and undervoltages.

A. Simulation setup

In the following, we assume the controllable DERs to be equipped with the following overvoltage protection.

Overvoltage protection scheme: We consider an overvoltage protection for PV plants, i.e., the plant is disconnected from the grid if the voltage goes above 1.06 pu, or stays above 1.05 pu for 10 minutes. The DER reconnects if the voltage remains below 1.05 pu for at least 1 minute. The disconnection scheme is inspired by the CENELEC EN50549-2 standard [32], and has been adjusted considering the voltage service limits used in this paper.

In the simulation, the voltage service limits are set to 1.05 and 0.95 p.u., respectively. The load and PV production profiles have a granularity of 1 second, i.e., active/reactive power consumption and maximum available active power for PV plants change every 1 second. The time horizon $T\tau$ is set to 1 hour, and the forecast update $\Delta\tau$ to 30 minutes. The reactive power setpoints update τ is set to 100 ms. We compare our proposed controller, based on Algorithm 1 (OGD-CCO), with: (a) a static Volt/Var control (VoltVar); and, (b) no control (ON/OFF).

[2]Data available at https://data.open-power-system-data.org/household_data/2020-04-15

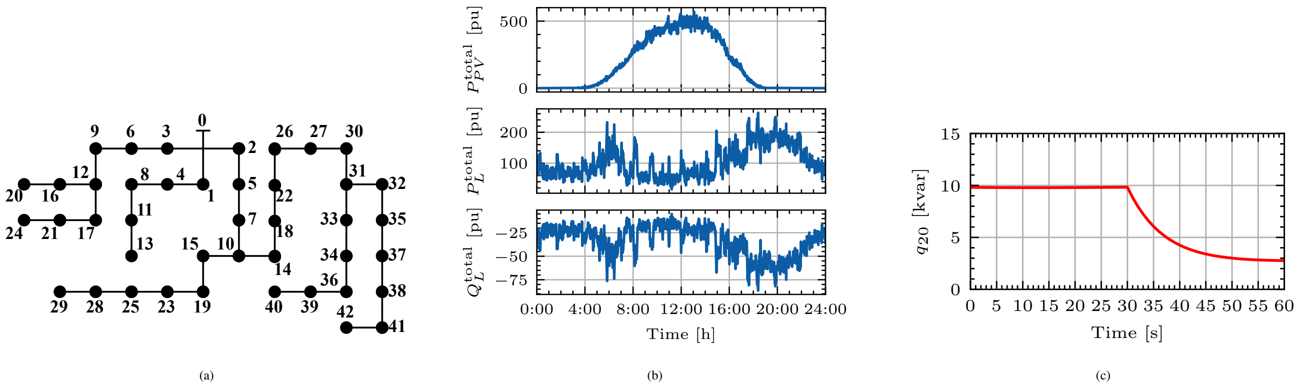

Fig. 4: (a) Low-voltage 42-nodes network, (b) aggregated non-controllable active power injections, and active/reactive power consumption, (c) reactive power setpoint update for controller at node 20 around hour 20:00.

a) Static Volt/Var control: It is inspired by the standard *IEEE Std 1547-2018*, with maximum reactive power consumed/absorbed set to 44% of the nominal power of the DER and reached for voltages 1.05/0.95 pu, respectively. The deadband ranges between 0.99 and 1.01 pu. Active power prioritization is implemented. Therefore, the maximum reactive power that can be produced or consumed corresponds to the minimum between 44% of the nominal apparent power s_g and the reactive power reserve of the inverter $\sqrt{s_g^2 - p_g^2}$, with p_g the active power injection of DER g.

b) No control: Set controller gains $\eta = \alpha = 0$, and reactive powers to 0.

B. Results

In Fig. 5, we illustrate the dynamics of the controllers associated with DER connected to two different nodes and the corresponding voltage magnitudes. We compare the voltage magnitudes resulting from the deployment of different controllers against the case without controllers and without overvoltage protection. We fixed $T_{\mathcal{T}}$ to 1 hour, i.e., the controller gains change every hour. It is clear that the VoltVar control overuses reactive power, as there is no need to control the voltages between hours 16:00 – 17:00, or after 22:00. The ON/OFF strategy sees large fluctuations in voltages due to constant connection and disconnection of DERs. Fig. 4c illustrates the reactive power setpoint update for the DER connected at node 20 at hour 20:00. In about 7 seconds, the reactive power setpoint varies with a magnitude of 5kvar, which we believe is reasonable. However, if the reactive power setpoints are ramp limited, this would not drastically affect the results since such large variations can occur only during change of hours, and for certain specific changes (in this scenario, at hours 8:00, 16:00, 18:00, 20:00, 21:00 and 22:00).

The cumulative distribution functions (CDF) for maximum and minimum voltages during the simulation are shown in Fig. 6. At each time t between hours h_1 and h_2, we pick the maximum and minimum voltages throughout the network and store them into two distinct vectors. We then plot the cumulative distribution functions of those vectors. For $\mathcal{T}_{0-24}$, i.e. for the entire duration of the simulation, our proposed method crosses the 1.05 p.u. line above 95% for the maximum voltage, and lower than 5% for the undervoltage. This means that the voltage constraints are satisfied at least 95% of the time, which is consistent with our choice of $\epsilon = 0.05$ and $\epsilon = 0.2$. We also show the CDF during two other intervals, between hours 7:00 – 8:00 for overvoltages and 18:00 – 19:00 for undervoltages. Notice that a larger ϵ allows for more voltage constraint violations. The VoltVar control sees overvoltages more than 10% of the time while performing similarly to our method for undervoltages. The ON/OFF strategy sees overvoltages more than 20% of the time.

Fig. 7 displays, from top to bottom, the energy lost in the lines, the energy lost because of active power curtailment, and the cumulative reactive energy usage for the different strategies considered in this work. The line losses are computed based on the line currents squared times the line resistances. Although the usage of reactive power is *practically free*, it induces larger line currents, hence larger power losses. We make a distinction between losses caused by active power curtailment and line losses since the former are covered by the network user while the latter are covered by the system operator. However, the system operator can in turn increase network tariffs to compensate for line losses due to overuse of reactive power compensation.

Our controller applies reactive power prioritization, which naturally induces active power curtailment if the DER injects a large amount of active power into the network. On the other hand, the VoltVar and ON/OFF strategies may experience active power curtailment because of prolonged overvoltage violations. Taking all these competing factor into consideration, the total energy loss is much more important for the ON/OFF strategy, while it is

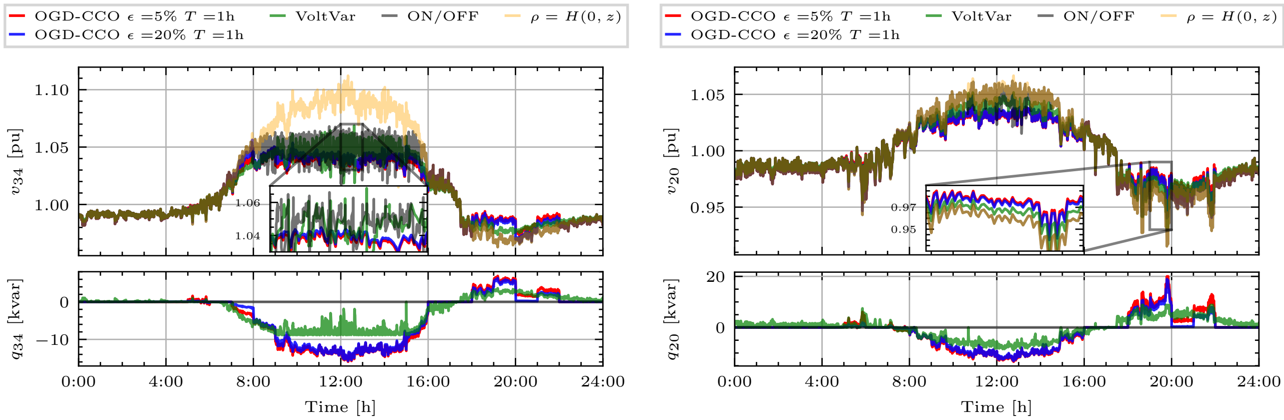

Fig. 5: Controller dynamics and voltage magnitudes for two given nodes: node 34 and node 20.

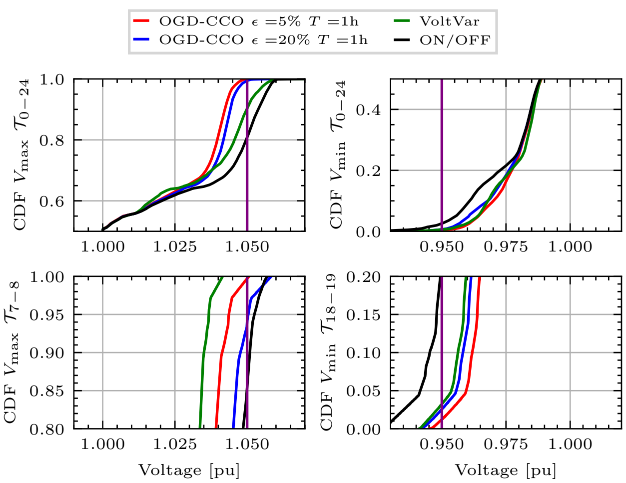

Fig. 6: Cumulative distribution function for the vectors $\mathbf{V}_{\max} = \{\max v_{i,k}\}_{i \in \mathcal{N}, k \in \mathcal{T}_{h1-h2}}$, and $\mathbf{V}_{\min} = \{\min v_{i,k}\}_{i \in \mathcal{N}, k \in \mathcal{T}_{h1-h2}}$, where $\mathcal{T}_{h1-h2}$ is the set of time indices between hours h_1 and h_2.

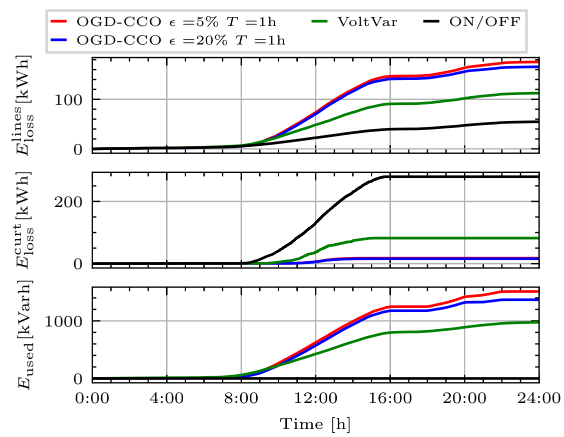

Fig. 7: Energy lost in the lines and because of curtailment, and reactive energy usage.

equivalent for our controller and the VoltVar control. One can see in Fig. 7 that the VoltVar control uses reactive power all day long, even when it is not needed (e.g. between hours 20:00 – 21:00), while our proposed method better manages the resources. One can also see that the parameter ϵ acts as a lever on the total usage of reactive power. If the reactive power is very expensive, and voltage violations are not extremely important, one could increase the value of ϵ to reduce the total usage of reactive energy.

In Fig. 8, we show the maximum duration of voltage violations. The vector $\Gamma_{\mathcal{V}}$ is built such that, if an overvoltage or undervoltage occurs in the network at a given time step $k\tau$, we count and add up every voltage violations for the subsequent time steps. When, at a subsequent time step, no voltage violation occurs, the total number of voltage violation is appended to the vector, and the counter is reset to 0. The vector $\Gamma_{\mathcal{V}}$ indicates the duration of voltage violations. This is an important number, since usually electrical devices can cope with short and limited over or under voltages, but may be damaged during prolonged, large excursions from nominal voltages. The parameter ϵ sets the maximum time the voltage can exceed the voltage limits. For our given $\Delta\tau$ = 30 minutes, and with $\epsilon = 5\%$, the maximum duration for voltage violation is 90 seconds, while for $\epsilon = 20\%$, it is 360 seconds.

Fig. 8 shows that a smaller ϵ leads to shorter voltage violations, while both ON/OFF and VoltVar strategies lead to substantially longer voltage violations.

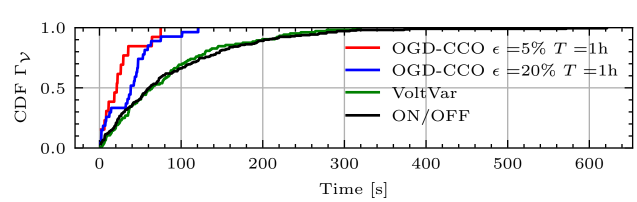

Fig. 8: Cumulative distribution function for voltage violations.

VII. Conclusion

We propose an incremental Volt/Var control strategy for voltage regulation in DNs. We show the stability of our controller, and introduce a methodology to compute the gains of our controller based on a chance-constrained formulation of an optimal reactive power flow problem. Our methodology only needs limited offline communications, i.e., the same controller gains are broadcast to individual controllers. Our chance-constrained formulation tackles uncertainties in power injections. Moreover, the feasibility issue of local Volt/Var control, i.e., if there is enough reactive power reserve to satisfy the voltage constraints given the architecture of the controller, is implicitly taken into account by allowing the system operator to tolerate a prescribed probability of voltage violations. Our method shows better performance compared to static Volt/Var curves with fixed parameters, and limited and short voltage violations that are consistent with the prescribed probability. Future works will investigate the combination of our fast-acting controller with slower traditional regulation devices.

References

[1] R. Walling, R. Saint, R. C. Dugan, J. Burke, and L. A. Kojovic, "Summary of distributed resources impact on power delivery systems," *IEEE Trans. on Power Delivery*, vol. 23, no. 3, pp. 1636–1644, 2008.

[2] M. S. Alam, F. S. Al-Ismail, A. Salem, and M. A. Abido, "High-level penetration of renewable energy sources into grid utility: Challenges and solutions," *IEEE Access*, vol. 8, pp. 190 277–190 299, 2020.

[3] J. McDonald, "Solar power impacts power electronics in the smart grid," *Power Electronics*, 2013.

[4] K. E. Antoniadou-Plytaria, I. N. Kouveliotis-Lysikatos, P. S. Georgilakis, and N. D. Hatziargyriou, "Distributed and decentralized voltage control of smart distribution networks: Models, methods, and future research," *IEEE Trans. on Smart Grid*, vol. 8, no. 6, pp. 2999–3008, 2017.

[5] P. Srivastava, R. Haider, V. J. Nair, V. Venkataramanan, A. M. Annaswamy, and A. K. Srivastava, "Voltage regulation in distribution grids: A survey," *Annual Reviews in Control*, vol. 55, pp. 165–181, 2023.

[6] A. Colot, Y. Chen, B. Cornélusse, J. Cortés, and E. Dall'Anese, "Optimal power flow pursuit via feedback-based safe gradient flow," *arXiv:2312.12267*, 2023.

[7] L. Ortmann, J. Maeght, P. Panciatici, F. Dörfler, and S. Bolognani, "Online feedback optimization for subtransmission grid control," *arXiv:2212.07795*, 2023.

[8] H. Zhu and H. J. Liu, "Fast local voltage control under limited reactive power: Optimality and stability analysis," *IEEE Trans. on Power Syst.*, vol. 31, no. 5, pp. 3794–3803, 2016.

[9] X. Zhou, M. Farivar, Z. Liu, L. Chen, and S. H. Low, "Reverse and forward engineering of local voltage control in distribution networks," *IEEE Trans. on Automatic Control*, vol. 66, no. 3, pp. 1116–1128, 2021.

[10] K. Baker, A. Bernstein, E. Dall'Anese, and C. Zhao, "Network-cognizant voltage droop control for distribution grids," *IEEE Trans. on Power Syst.*, vol. 33, no. 2, pp. 2098–2108, 2018.

[11] P. Jahangiri and D. C. Aliprantis, "Distributed Volt/VAr control by PV inverters," *IEEE Trans. on Power Syst.*, vol. 28, no. 3, pp. 3429–3439, 2013.

[12] M. Farivar, X. Zho, and L. Chen, "Local voltage control in distribution systems: An incremental control algorithm," in *2015 IEEE International Conference on Smart Grid Communications (SmartGridComm)*, 2015, pp. 732–737.

[13] J. Wei, S. Gupta, D. C. Aliprantis, and V. Kekatos, "A chance-constrained optimal design of Volt/VAR control rules for distributed energy resources," in *2023 North American Power Symposium (NAPS)*, 2023, pp. 1–6.

[14] F. U. Nazir, B. C. Pal, and R. A. Jabr, "A two-stage chance constrained volt/var control scheme for active distribution networks with nodal power uncertainties," *IEEE Trans. on Power Syst.*, vol. 34, no. 1, pp. 314–325, 2019.

[15] S. Karagiannopoulos, P. Aristidou, and G. Hug, "Data-driven local control design for active distribution grids using off-line optimal power flow and machine learning techniques," *IEEE Trans. on Smart Grid*, vol. 10, no. 6, pp. 6461–6471, 2019.

[16] A. Eggli, S. Karagiannopoulos, S. Bolognani, and G. Hug, "Stability analysis and design of local control schemes in active distribution grids," *IEEE Trans. on Power Syst.*, vol. 36, no. 3, pp. 1900–1909, 2020.

[17] S. Gupta, A. Mehrizi-Sani, S. Chatzivasileiadis, and V. Kekatos, "Deep learning for scalable optimal design of incremental Volt/VAR control rules," *IEEE Control Systems Letters*, vol. 7, pp. 1957–1962, 2023.

[18] S. Gupta, V. Kekatos, and S. Chatzivasileiadis, "Optimal design of Volt/VAR control rules of inverters using deep learning," *arXiv:2211.09557*, 2024.

[19] Z. Yuan, G. Cavraro, M. K. Singh, and J. Cortés, "Learning provably stable local Volt/Var controllers for efficient network operation," *IEEE Trans. on Power Syst.*, vol. 39, no. 1, pp. 2066–2079, 2024.

[20] P. Serna Torre and P. Hidalgo-Gonzalez, "Decentralized optimal power flow for time-varying network topologies using machine learning," *Electric Power Systems Research*, vol. 212, p. 108575, 2022.

[21] A. Nemirovski and A. Shapiro, "Convex approximations of chance constrained programs," *SIAM Journal on Optimization*, vol. 17, no. 4, pp. 969–996, 2007.

[22] G. Scutari, F. Facchinei, L. Lampariello, and P. Song, "Parallel and distributed methods for nonconvex optimization," in *2014 IEEE International Conference on Acoustics, Speech and Signal Processing (ICASSP)*, 2014, pp. 840–844.

[23] S. Bolognani and S. Zampieri, "On the existence and linear approximation of the power flow solution in power distribution networks," *IEEE Trans. on Power Syst.*, vol. 31, no. 1, pp. 163–172, 2015.

[24] C. Wang, A. Bernstein, J.-Y. Le Boudec, and M. Paolone, "Explicit conditions on existence and uniqueness of load-flow solutions in distribution networks," *IEEE Trans. on Smart Grid*, vol. 9, no. 2, pp. 953–962, 2016.

[25] ——, "Existence and uniqueness of load-flow solutions in three-phase distribution networks," *IEEE Trans. on Power Syst.*, vol. 32, no. 4, pp. 3319–3320, 2017.

[26] E. Dall'Anese and A. Simonetto, "Optimal power flow pursuit," *IEEE Trans. on Smart Grid*, vol. 9, no. 2, pp. 942–952, 2016.

[27] N. Li, G. Qu, and M. Dahleh, "Real-time decentralized voltage control in distribution networks," in *2014 52nd Annual Allerton Conference on Communication, Control, and Computing (Allerton)*, 2014, pp. 582–588.

[28] M. E. Baran and F. F. Wu, "Network reconfiguration in distribution systems for loss reduction and load balancing," *IEEE Trans. on Power delivery*, vol. 4, no. 2, pp. 1401–1407, 1989.

[29] M. Farivar, L. Chen, and S. Low, "Equilibrium and dynamics of local voltage control in distribution systems," in *52nd IEEE Conference on Decision and Control*, 2013, pp. 4329–4334.

[30] V. Kekatos, L. Zhang, G. B. Giannakis, and R. Baldick, "Voltage regulation algorithms for multiphase power distribution grids," *IEEE Trans. on Power Syst.*, vol. 31, no. 5, pp. 3913–3923, 2015.

[31] D. Sarajlić and C. Rehtanz, "Low voltage benchmark distribution network models based on publicly available data," in *2019 IEEE PES Innovative Smart Grid Technologies Europe (ISGT-Europe)*, 2019, pp. 1–5.

[32] "Requirements for generating plants to be connected in parallel with distribution networks – Part 2: connection to a MV distribution network – generating plants up to and including type B," *CENELEC*, pp. 1–84, 2019.